



Optimal Design of MR Brake with Different Shapes of the Brake Envelop

Quoc Hung Nguyen

Professor, Department of Mechanical Engineering, Industrial University of Ho Chi Minh City.

ABSTRACT

In design of magneto-rheological brake (MRB), it is well-known that the shape of the brake envelopes significantly affects to performance characteristics of the brake. In this study, different shapes of MR brake envelop such as rectangular and polygon shape of the envelope are considered from which the most suitable shape is identified. After an introduction of MRBs with different envelop shapes, the braking torque of the brake is derived based on Bingham-plastic behavior of the magneto-rheological fluid (MRF). Optimal design of the MRB with different envelop shapes is then performed. The optimization problem is to find optimal value of significant geometric dimensions of the MRBs that can produce a required braking torque while their mass is minimized. A finite element analysis integrated with an optimization tool is employed to obtain optimal solutions of the MRBs. From the results, the most suitable shape of the brake envelop is identified.

Keywords: Magnetorheological Fluid (MRF), MR Brake, Optimal Design

***Corresponding author E-mail:** khoi280986@gmail.com

1. INTRODUCTION

As well known, the magnetorheological fluid (MRF) is a suspension of particles, which can be magnetized, and exhibit fast, strong, and reversible changes in their rheological properties when a magnetic field is applied. Therefore, MRF holds great potential in many applications that require an electromechanical interface such as clutches brakes, valves, dampers and robotics (Wang and Meng, 2001; Muhammad et al., 2006).

There have been a large number of researches on development of brakes featuring MRF (MRB) in many applications. Many types of MRBs have been proposed and evaluated such as: disk type MRB (Rabinow, 1951; An and Kwon, 2003; Park et al., 2006; Liu et al., 2006), drum-type MRBs (Huang J et al., 2002; Smith A L et al, 2007), hybrid-type MRB (a combination of disc-type and drum type MRB) with T-shaped rotor MRBs (Nguyen and Choi, 2012). Nguyen et al. have performed researches on optimal design of different types of MRB (Nguyen and Choi, 2012). The objective of the optimization is to maximize braking torque of the MRBs constrained in a specific volume. The optimal solutions of the MRBs constrained in different volumes were then obtained and presented. From the results, hints on selection of MRBs type were also proposed. Although there have been a large number of researches on design and application of MRBs and various types of MRB configuration have been proposed, the shape of the MRB envelop (housing) was not taken into consideration. Generally, in previous researches, the MRB envelope often had a rectangular shape. Obviously, the rectangular envelope is convenient in design and manufacturing. However, the rectangular shape of the envelope causes an uneven distribution of magnetic density resulting in local “bottom-neck” problems of the MRB magnetic flow, which reduces braking torque of the MRBs. In addition, the rectangular shapes of the envelope may result in a heavy weight of the MRBs.

This research focuses on optimal design of the MRBs considering different shapes of the

brake envelop. The shapes of MRB envelop considered in this study includes conventional rectangular shape, 5-segment polygonal shape and 7-segment polygonal shape. This work considers only the disc-type MRBs. The results can be extended to other types of MRBs. After the introduction of MRBs with different envelop shapes, braking torque of the brake is derived based on Bingham-plastic behavior of the magneto-rheological fluid. Optimal design of the MRB with different envelop shapes is then considered. The optimization problem is to find optimal value of significant geometric dimensions of the most compact MRB that can produce a required braking torque. A finite element analysis integrated with an optimization tool is employed to obtain optimal solutions of the MRBs. From the results, the most suitable shape of the brake envelop is identified.

2. MATERIALS AND METHODS

2-1 Mr Brakes Featuring Different Shapes Of The Brake Envelop

In this section, a disc-type MRB featuring different shapes of the envelop is considered and its braking torque is analyzed based on Bingham-plastic behavior of MRFs. Fig. 1 shows a typical configuration of a disc-type MRB with rectangular-shaped envelop (shortly called rectangular MRB) . The rotor of the brake is very thin compared to its radius, which is referred as a rotary disc. When a current is applied to the coil, a magnetic field is generated; the MRF at the end-faces of the disc is energized and becomes solid-like. The shear friction between the rotating disc and the solidified MRF provides a braking force to slow down and stop the shaft. The shear friction between the rotating disc and the solidified MRF provides a braking force to slow down and stop the shaft. Significant geometric dimensions of the MRBs are also shown in the figure.

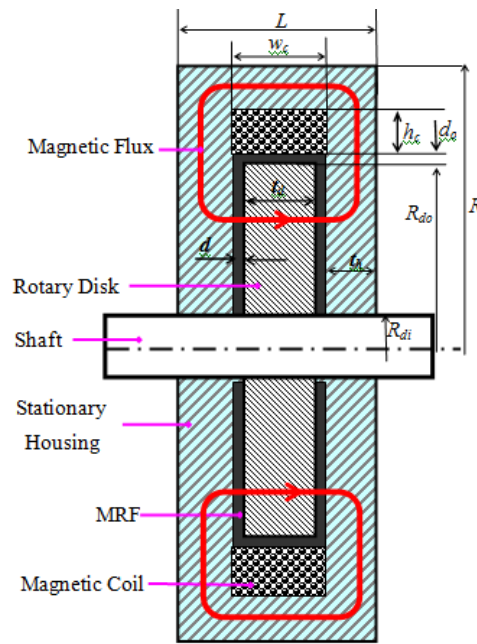


Figure 1. Configuration of a disc-type MRB with rectangular envelop

It is known that the rectangular envelope is convenient in design and manufacturing of the MRB. However, in the rectangular-shaped envelope, the distribution of magnetic density is very uneven resulting in local “bottom-neck” problems of magnetic flow of the MRB, which reduces performance characteristics of the MRBs. In order to solve the problems of the MRB with rectangular-shaped envelop and the MRBs with polygonal shaped envelop are proposed in this study. Fig. 2 shows the proposed disc-type MRB with 5-segment polygonal envelop (shortly referred as 5-seg-polygonal MRB). As shown in the figure, the outer boundary of the envelop consists of five segments: the first one is in horizontal direction determined by the outer housing thickness t_{h1} and the outer housing radius R_1 (point P_1), the second one determined by the housing thickness and the housing radius at the outer radius of the coil t_{h2} and R_2 (point P_2), the third one determined by the housing thickness and the housing radius at the outer radius of the disc t_{h3} and R_3 (point P_3), the fourth one determined by t_{h4} and R_4 which are respectively the housing thickness and the housing radius at point P_4 located between the outer radius and inner radius of the disc, and the fifth one determined the inner housing

thickness and the shaft radius t_{hs} and R_s (point P_5). It is observed that, with the polygonal shape of the envelop, the cross-sectional area of the MRB magnetic circuit can be flexibly designed so that the distribution of magnetic density is more uniform to partially avoid the local “bottom-neck” problems of magnetic flow. Significant geometric dimensions of the brake are also shown in Fig. 2.

In order to more flexibly design cross-sectional area of the magnetic circuit, the MRB with 7-segment polygonal envelop (shortly referred as 5-seg-polygonal MRB) is proposed and shown in Fig. 3.

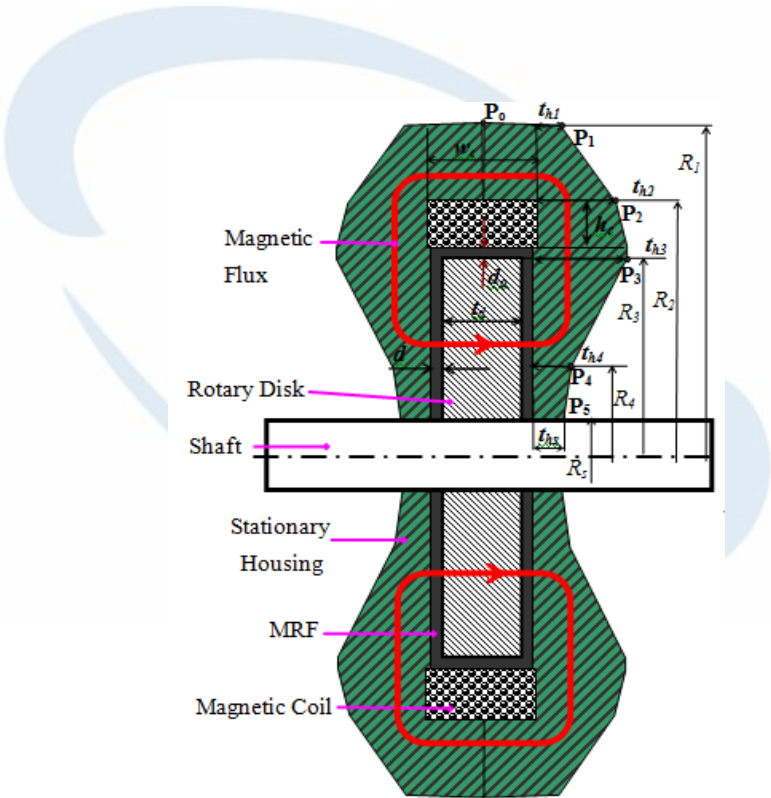


Figure 2. Configuration of a disc-type MRB with 5-segment polygonal envelop

As shown in the figure, the polygonal shape of the MRB envelop consists of 7 segments correspondingly determined by $P_1, P_2, P_3, P_4, P_5, P_6$ and P_7 , in which P_1, P_2, P_3, P_4 and P_5 are similar to those of the 5-segment envelop. The point P_6 is added between P_1 and P_2 while point P_7 is added between P_4 and P_5 . Significant geometric dimensions are also shown in Fig. 3.

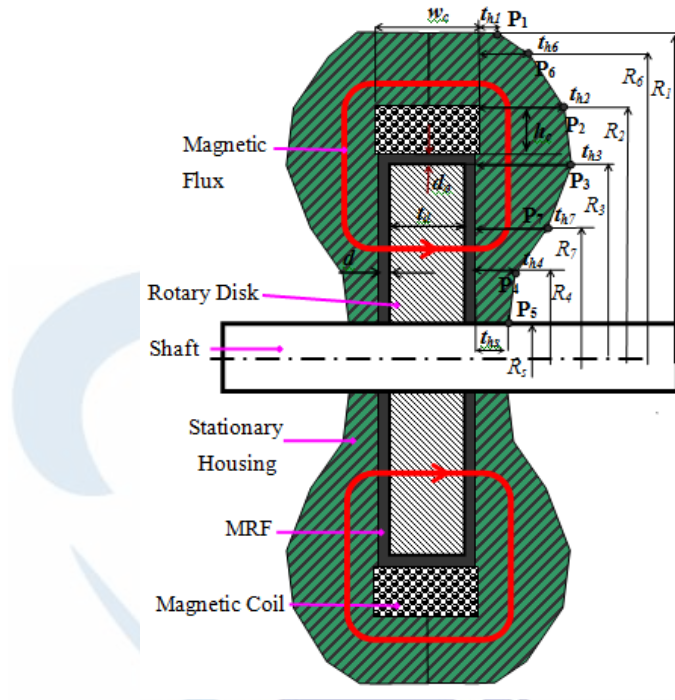


Figure 3. Configuration of a disc-type MRB with 7-segment polygonal envelop

2-2 MRBs Featuring Different Shapes Of The Brake Envelop

In design of MRBs, the most important issue should be taken into account is the maximum braking torque. The maximum braking torque of MRBs should be greater than a required value. By assuming that MRFs rheologically behave as Bingham plastic fluids and by the assumption of linear velocity profile in the MRF ducts of the brake, the induced braking torque and the off-state force of a disc-type MRB are respectively determined by

$$T_d = \frac{\pi\mu_d R_{do}^4}{d} \left[1 - \left(\frac{R_{di}}{R_{do}} \right)^4 \right] \Omega + \frac{4\pi\tau_{yd}}{3} (R_{do}^3 - R_{di}^3) + 2\pi R_{do}^2 t_d (\tau_{y0} + \mu_0 \frac{\Omega R_{do}}{d_o}) + 2T_{or} \quad (1)$$

$$T_{d0} = \frac{\pi\mu_0 R_{do}^4}{d} \left[1 - \left(\frac{R_{di}}{R_{do}}\right)^4\right] \Omega + \frac{4\pi\tau_{y0}}{3} (R_{do}^3 - R_{di}^3) + 2\pi R_{do}^2 t_d (\tau_{y0} + \mu_0 \frac{\Omega R_{do}}{d_o}) + 2T_{or} \quad (2)$$

where R_{di} and R_{do} are the inner and outer radius of the disc, d is the gap size of the end-face MRF ducts between the disc and the housing, d_o is the gap size of the annular MRF duct at the outer cylindrical face of the disc, t_d is the thickness of the disc, Ω is the angular velocity of the rotor, μ_d is the post yield viscosity and τ_{yd} is the yield stress of the MRF in the end-face ducts, τ_{y0} and μ_0 are the zero-field yield stress and viscosity of the MRF, and T_{or} is the friction torque between the shaft of the brake and the o-ring. It is noted that τ_{yd} and μ_d are fluid properties, their values depend on the exerted magnetic flux density across the ducts of MRF.

The o-ring friction torque T_{or} can be approximately calculated by (Brian, 2005)

$$T_{or} = (f_c L_c + f_h A_r) R_s \quad (3)$$

where L_c is the length of seal rubbing surface of the brake shaft (the shaft circumference), $L_c = 2\pi R_s$, f_c is friction per unit length of the shaft circumference due to o-ring compression depending on percentage of seal compression and hardness of the o-ring material, f_h is the o-ring friction force due to fluid pressure acting on a unit projected area of the brake shaft o-ring and A_r is the seal projected area. It is noted that in haptic application, the angular velocity of the brake shaft is very small and the pressure due to MRF acting on the o-rings is very low which can be neglected, $f_h \cong 0$. It is also noteworthy that the pressure built in the MRF duct of the brake is very small, so a high compression of the o-rings for sealing is not required. In this study, the 70-durometer rubber o-ring is used and the compression of the o-ring is set by 10%. In this case the coefficient f_c is around 125N/m.

Another issue should be taken into account in design of MRBs is their mass. It is obvious that the mass of the MRBs should be as small as possible to reduce the MRB size and cost. Generally, the MRB mass can be approximately calculated by

$$m_b = V_d \rho_d + V_h \rho_h + V_s \rho_s + V_{MR} \rho_{MR} + V_{bob} \rho_{bob} + V_c \rho_c \quad (4)$$

where V_d , V_h , V_s , V_{MR} , V_{bob} and V_c are respectively the geometric volume of the discs, the housing, the shaft, the MRF, the bobbin and the coil of the brake. These parameters are functions of geometric dimensions of the MRB structures, which vary during the optimization process. ρ_d , ρ_h , ρ_s , ρ_{MR} , ρ_{bob} and ρ_c are density of the discs, the housing, the shaft, the MRF, the bobbin and the coil material, respectively.

Taking the above mentions into consideration, the optimization design problem of the MRBs in this study can be summarized as follows: Find optimal value of significant dimensions of the MRB so that its maximum braking torque determined by Eq. (1) is greater than a required braking torque. In addition, the brake mass determined by Eq. (4) should be minimized.

It is assumed that the commercial silicon steel is used for magnetic components of the MRB such as MRB housing and disc. The coil wires are sized as 21-gage (diameter = 0.511mm). During the optimization process, a maximum current of 2.5A is applied the coil. In this work, the commercial MR fluid: MRF132-DG (moderate yield stress) made by Lord Corporation is used. Rheological properties of the MRFs can be estimated by the following equation (Nguyen et al., 2012; Zubieta et al., 2009)

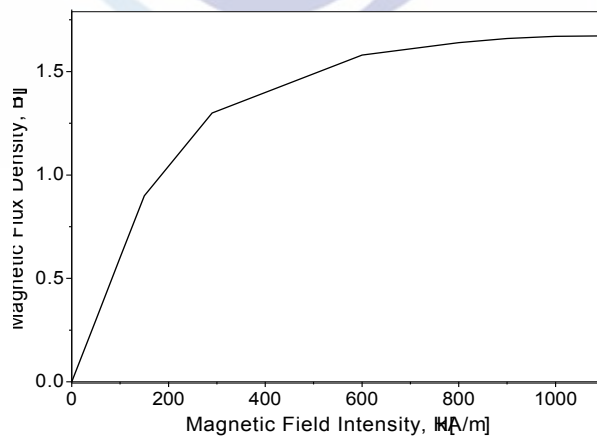
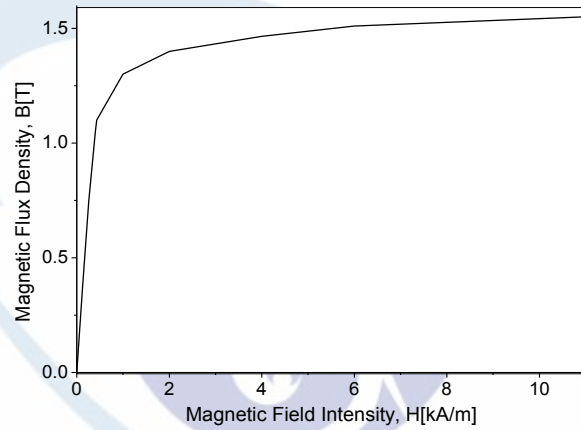
$$Y = Y_{\infty} + (Y_0 - Y_{\infty})(2e^{-B\alpha_{SY}} - e^{-2B\alpha_{SY}}) \quad (5)$$

where Y stands for a rheological parameters of MRF such as yield stress, post yield viscosity, fluid consistency and flow behavior index. The value of Y tends from the zero-applied field value Y_0 to the saturation value Y_{∞} . α_{SY} is the saturation moment index of the Y parameter. B is the applied magnetic density. The Magnetic properties of the brake components are given in Table 1 and Fig. 4 The rheological parameters of MRFs determined from experimental results using curve fitting method are: $\mu_0 = 0.1 \text{ pa.s}$; $\mu_{\infty} = 3.8 \text{ pa.s}$; $\alpha_{s\mu} = 4.5 \text{ T}^{-1}$ $\tau_{y0} = 15 \text{ pa}$;

$$\tau_{y\infty} = 40000 \text{ pa}; \quad \alpha_{st_y} = 2.9T^{-1}$$

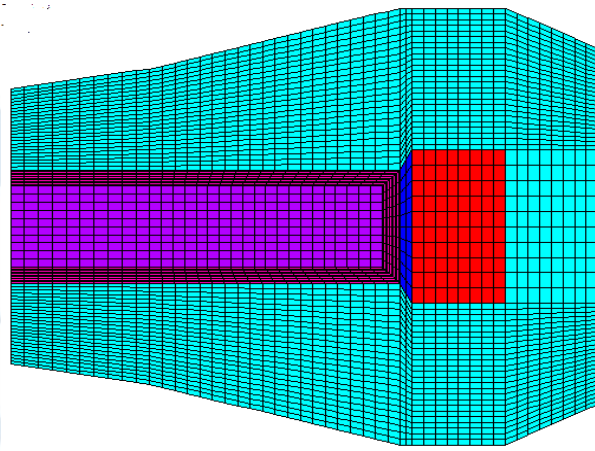
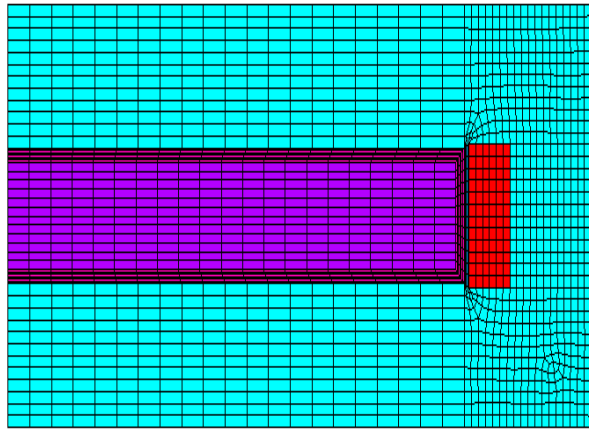
Table 1. Magnetic properties of the MRBs' components

Material	Relative Permeability	Saturation Flux Density
Silicon Steel	B-H curve (Fig. 5a)	1.55 Tesla
Copper	1	
MRF132-DG	B-H curve (Fig. 5b)	1.65 Tesla
Nonmagnetic Steel	1	x



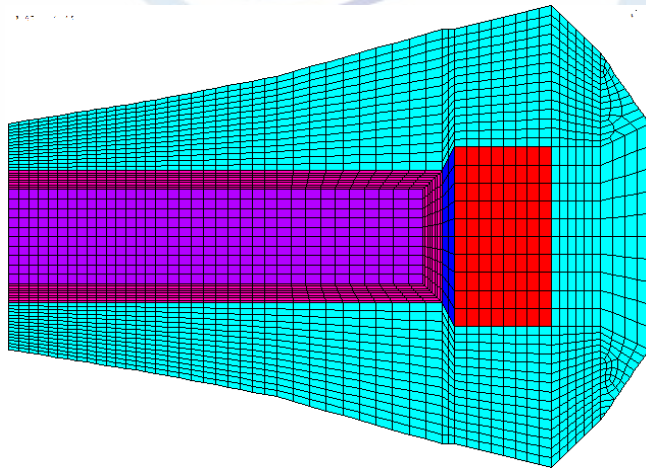
(a) B-H curve of silicon steel (b) B-H curve of MRF-132DG

Figure 4. Magnetic properties of silicon steel and MR fluid



(a) rectangular-shaped envelop

(b) 5-segment polygonal shaped envelop



(c) 7-segment polygonal shaped envelop

Figure 5. Finite element models to solve magnetic circuit of the MRBs

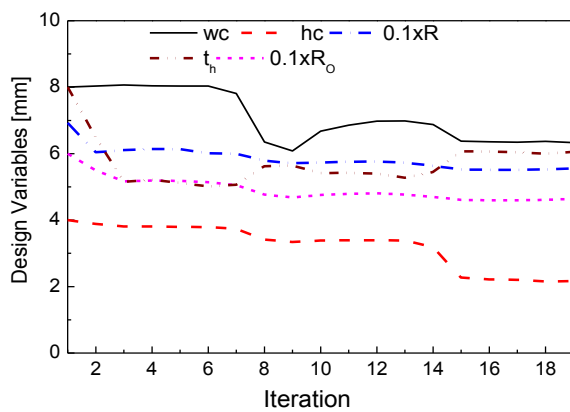
In order to predict the yield stress and post yield viscosity using Eq. (5), firstly, the magnetic density across the MR gap is calculated using FEA. The finite element models, at initial value of design variables, using 2D-axisymmetric couple element (plane 13) of commercial ANSYS software to solve magnetic circuits of the MRBs are shown in Fig. 5 It is noted that geometric dimensions of the MRBs is altered during optimization process, so the meshing size is defined by the number of elements per line and this element number is unchanged during the optimization process.

In the optimization, the coil height h_c , the coil width w_c , the housing thickness t_{hi} and radius R_i at the point P_s of the MRB envelop are considered as design variables. It is noteworthy that optimal value of the MRF gap size, d , is not affected by the envelop shape. Therefore, in this study, the MRF gap size is not considered as a design variable and empirically set by $0.8mm$. In order to obtain the optimal solution, a FEA code integrated with an optimization tool is employed. In this study, the first order method with golden section algorithm of ANSYS optimization tool is used. The detailed procedure to obtain the optimal solution of MR fluid devices based on FEA has been mentioned in several researches (Nguyen et al., 2007).

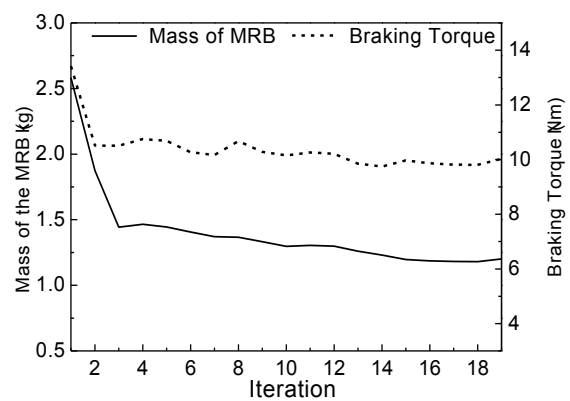
3. RESULTS AND DISCUSSION

In this section, the optimal solutions of the above MRBs are obtained and presented. Fig. 6, Fig. 7, and Fig. 8 respectively show the optimal solution of the rectangular, the 5-seg-polygon and the 7-seg-polygon MRB featuring MRF-132-DG. The braking torque is constrained to be greater than $10Nm$ and the convergence rate is set by 0.1%. It is noteworthy that the shaft radius in this case is set by $R_s=6mm$ considering the strength of the shaft. As shown in Fig. 6a and 6b, the optimization is converged after 19 iterations. The optimal results at the 19th iteration are (mm): $w_c=6.35$, $h_c=2.2$, $t_h=6$, $R_o=46$ and $R=55$. At the optimum, the braking torque can reach up to $10kN$ as constrained and the minimum mass is $1.21kg$. Fig. 6c shows the magnetic

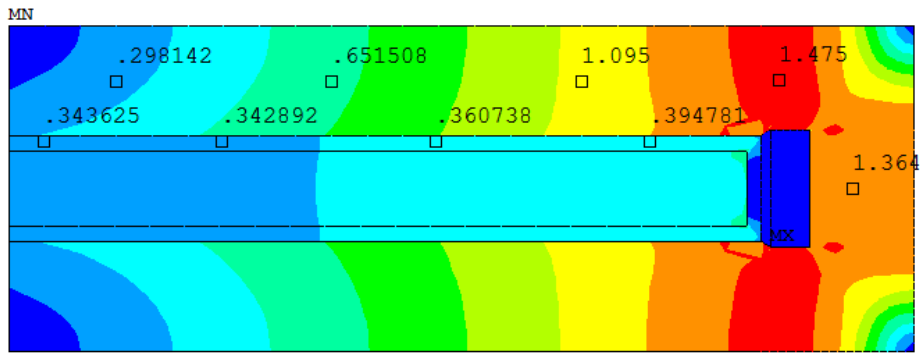
distribution of the optimized rectangular MRB. As shown in the figure, the magnetic distribution in the housing is very different. The magnetic density near the coil almost reaches to the magnetic saturation of the housing material while that near the shaft is very small. For the 5-seg-polygon MRB, from Fig. 7a and 7b, it is observed that the convergence occurs at the 21st iteration at which the optimal results are (mm): $w_c=6.8$, $h_c=2.2$, $t_{h1}=5.5$, $t_{h2}=6$, $t_{h3}=5.6$, $t_{h4}=2.6$, $t_{hs}=2.5$, $R_1=57$, $R_2=51.6$, $R_3=48$ and $R_4=25.5$. At the optimum, the braking torque can reach up to 10kN as constrained and the minimum mass is 1.055kg. It is seen that the mass of the optimized 5-seg-polygon MRB is significantly reduced compared to that of the rectangular one. It is also shown in Fig. 7c that the magnetic distribution in the housing of the optimized 5-seg-polygon MRB is much more uniform than that of the rectangular one. For the 7-seg-polygon MRB, from Fig. 8a and 8b, it is observed that the convergence occurs at the 27th iteration at which the optimal results are (mm): $w_c=6.5$, $h_c=2.3$, $t_{h1}=4.7$, $t_{h2}=5.7$, $t_{h3}=5.8$, $t_{h4}=2.2$, $t_{hs}=2.05$, $t_{h6}=5$, $t_{h7}=3.5$, $R_1=56.9$, $R_2=51.5$, $R_3=47.8$, $R_4=24$, $R_6=54$ and $R_7=34$. At the optimum, the braking torque can reach up to 10kN as constrained and the minimum mass is 1.03kg. It is seen that the mass of the optimized 7-seg-polygon MRB is almost equal to that of the 5-seg-polygon MRB one. It is clearly shown from Fig. 8c that the magnetic distribution in the housing of the optimized 7-seg-polygon is a little bit more uniform than that of the 5-seg-polygon MRB.



(a) design variables



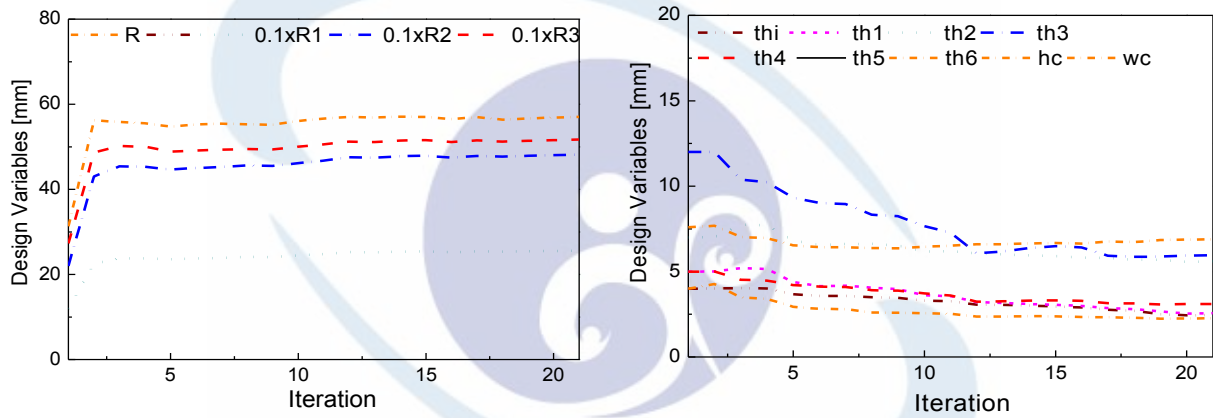
(b) braking torque and mass



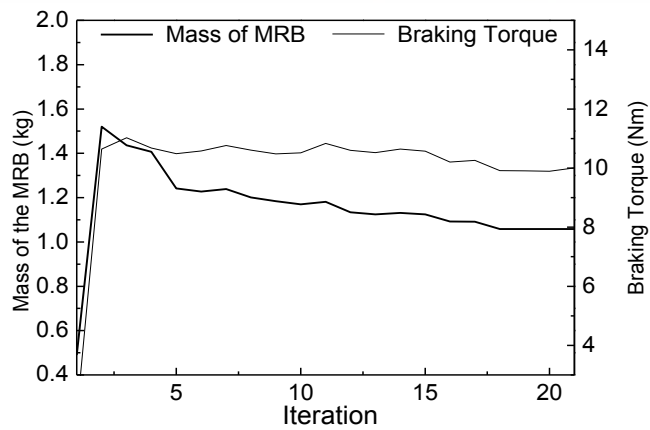
(c) magnetic flux density at the optimum

Figure 6. Optimization solution of the rectangular MRF-132-DG brake, braking torque \geq

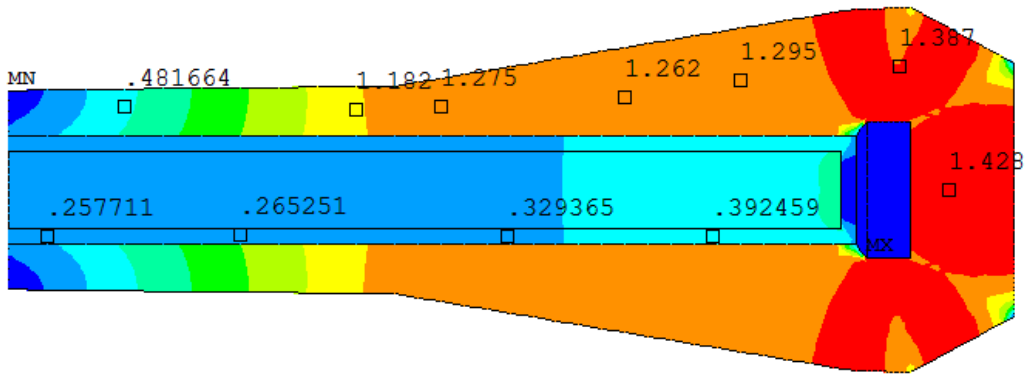
10Nm



(a) design variables

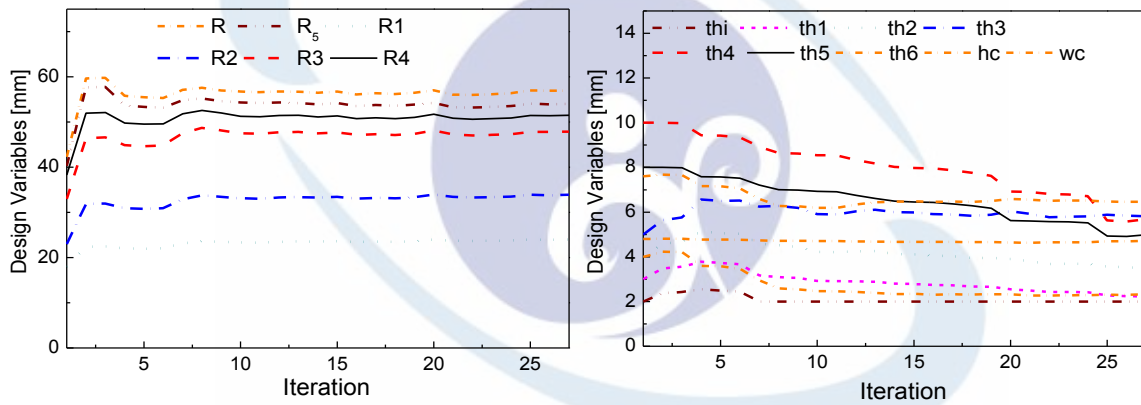


(b) braking torque and maximum MR fluid temperature

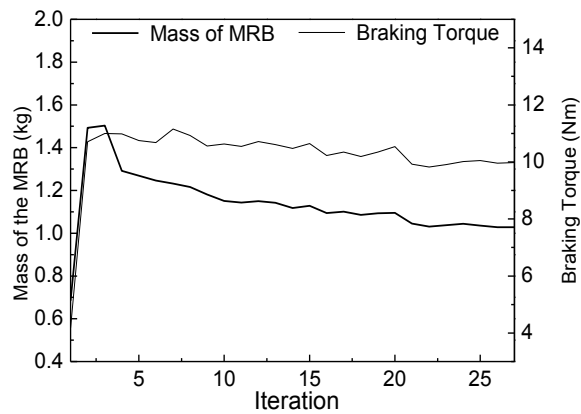


(c) magnetic flux density at the optimum

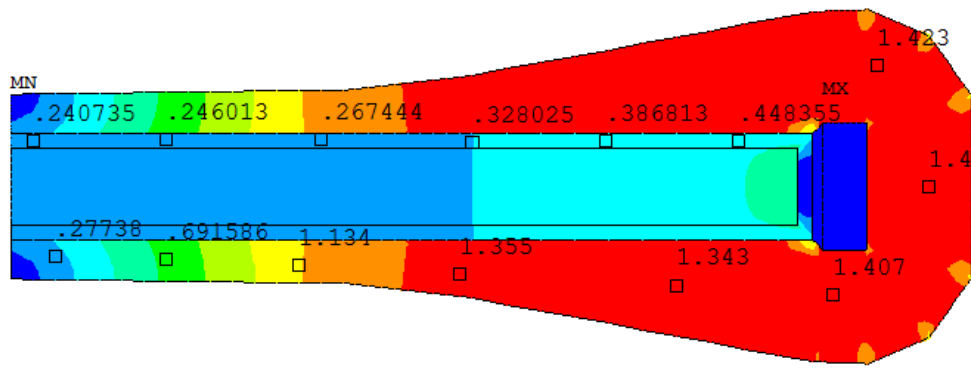
Figure 7. Optimization solution of the 5-segment polygon MRF-132-DG brake, braking torque $\geq 10\text{Nm}$



(a) design variables



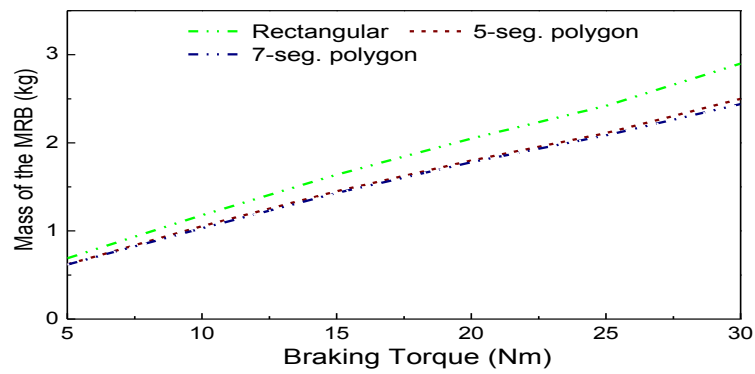
(b) braking torque and maximum MR fluid temperature



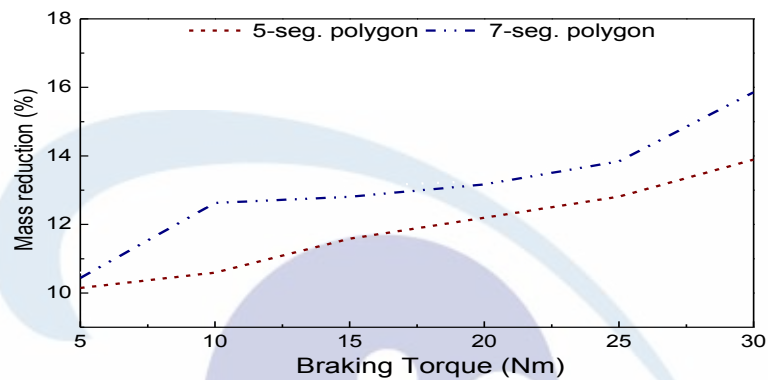
(c) magnetic flux density at the optimum

Figure 8. Optimization solution of the 7-segment polygon MRF-132-DG brake, braking torque $\geq 10Nm$

Fig. 9 shows the mass of optimized MRBs with different values of the constrained maximum braking torque. Noteworthily, by considering the strength of the shaft, the shaft radius is chosen corresponding to the constrained braking torque $T_{d,max}$ as follows: $R_s=6mm$ for $5Nm \leq T_{d,max} \leq 10Nm$; $R_s=8mm$ for $10Nm < T_{d,max} \leq 20Nm$; $R_s=10mm$ for $20Nm < T_{d,max} \leq 30Nm$. From Fig. 9a, it is found that the mass of the optimized 5-seg-polygon and the 7-seg-polygon are very close to each other and significantly smaller than that of the rectangular one at different values of the constrained braking torque. In order to observe the results more clearly, the mass reduction percentage of the 5-seg-polygon and 7-seg-polygon compared to the rectangular one are obtained and presented in Fig. 9b. It is seen from the figure that the mass reduction percentage of the 5-seg-polygon and 7-seg-polygon MRB (compared to the rectangular MRB) tends to increase with the increase of the constrained braking torque. For a constrained braking torque of $5Nm$, the mass reduction percentage of the 5-seg-polygon MRB is around 10% while it is increased up to 14% for a constrained braking torque of $30Nm$. It is also found that the difference between the mass reduction percentage of the 5-seg-polygon and the 7-seg-polygon MRB is not more than 2.4%.



(a) mass vs. braking torque



(b) mass reduction vs. braking torque

Figure 9. Mass of the optimized MRBs featuring MRF-132-DG as a function of maximum braking torque

From the above, it can be concluded that characteristics of MRBs are significantly affected by the shape of the MRB envelop. The mass of conventional rectangular MRBs can be significantly reduced by using a 5-seg-polygon envelop. It is also found that by using a polygon envelop with more control points, it is more flexibly to design cross-sectional areas of magnetic circuit of the MRBs and the mass of brakes can be more reduced. However, when the number of control points is sufficient the mass of MRBs reaches to a saturation. It is shown that the difference between the mass reduction of 5-seg-polygon and 7-seg-polygon MRB is not more than 2.4%.

4. CONCLUSION

In this research work, different shapes of MR brake envelop such as rectangular and polygon shape of the envelope were considered from which the most suitable shape is identified. In order to do this, optimal design of the MR brakes with different shapes of the envelop were performed. The objective of the optimization is to minimize the mass of the MR brakes while their braking torque, which is obtained based on Bingham-plastic behavior of the MRF, is constrained to be greater than a required value. A finite element analysis integrated with an optimization tool was employed to obtain optimal solutions of the MRBs. The results showed that the mass of conventional rectangular MRBs can be significantly reduced by using a 5-seg-polygon envelop. It was also found that the more control points is used for the polygon envelop, the more mass reduction of the MR brakes can be obtained. However, when the number of control points is sufficient the mass of MRBs reaches to a saturation. It was shown that the difference between the mass reduction percentage of 5-seg-polygon and 7-seg-polygon MR brakes is not more than 2.4%.

5. ACKNOWLEDGEMENT

This work was supported by the Vietnam National Foundation for Science and Technology Development (NAFOSTED) under grant no. 107. 04. 2011. 07.

REFERENCES

- An, J. and Kwon, D. S., 2003, "Modeling of a magnetorheological actuator including magnetic hysteresis," *Journal of Intelligent Material Systems and Structure* , Vol. 14 (9), pp. 541-550.
- Brian, E. S., 2005, "Research for dynamic seal Friction modeling in linear motion hydraulic Psston applications," *Master of Science thesis*, University of Texas at Arlington, USA.

- Huang, J., Zhang, J. Q., Yang, Y. and Wei, Y. Q., 2002, "Analysis and design of a cylindrical magnetorheological fluid brake," *Journal of Materials Processing Technology*, Vol. 129, pp. 559-562.
- Liu, B., Li, W. H., Kosasih, P. B. and Zhang, X. Z., 2006, "Development of an MR-brake-based haptic device," *Smart Materials and Structures*, Vol. 15, pp. 1960-1969.
- Muhammad A., Yao, X.L., Deng, J.C., 2006, "Review of magnetorheological (MR) fluids and its applications in vibration control," *Journal of Marine Science and Application*, Vol. 5, pp. 17-29.
- Nguyen, Q. H., Han, Y. M., Choi, S. B. and Wereley, N. M. 2007, "Geometry optimization of MR valves constrained in a specific volume using the finite element method," *Smart Materials and Structures*, Vol. 16, pp. 2242-2252.
- Nguyen, Q. H. and Choi, S. B., 2012, "Optimal design of a novel hybrid MR brake for motorcycles considering axial and radial magnetic flux," *Smart Materials and Structures*, Vol. 21(5), pp. 0964-1762.
- Nguyen, Q. H. and Choi, S. B., 2012, "Selection of magnetorheological brake types via optimal design considering maximum torque and constrained volume," *Smart Materials and Structures*, Vol. 21(1), pp. 0964-1726.
- Nguyen, Q. H., Choi, S. B., Lee, Y. S. and Han, M. S., 2012, "Optimal design of a new 3D haptic gripper for telemanipulation," *Featuring Magnetorheological Fluid Brakes*, pp. 0964-1726.
- Park, E. J., Stoikov, D., Luz, L. F. and Suleman, A., 2006, "A performance evaluation of an automotive magnetorheological brake design with a sliding mode controller." *Mechatronics*, Vol. 160, pp. 405-416
- Rabinow J 1951 Magnetic fluid torque and force transmitting device. *US patent 2,575,360*.
- Smith, A. L., Ulicny, J. C. and Kennedy, L. C., 2007, "Magnetorheological fluid fan drive for trucks," *Journal of Intelligent Material Systems and Structures* , Vol. 18 (12) , pp. 1131-1136.
- Wang, J., Meng, G., 2001, "Magnetorheological fluid devices: principles, characteristics and applications in mechanical engineering," *Journal of Materials: Design and Applications*, Vol. 215, pp. 165-74.
- Zubieta, M., Eceolaza, S., Elejabarrieta, M. J. and Bou-Ali, M. M., 2009, "Magnetorheological fluids: characterization and modeling of magnetization," *Smart Materials and Structures* ,Vol. 18, pp. 1-6.